Metallic conductivity versus charge disproportionation in the C_{60} complexes with noninteger average charge on fullerene

Dmitri V. Konarev,*[a] Salavat S. Khasanov,[b] Manabu Ishikawa,[c] Evgeniya I. Yudanova,[a] Artem F. Shevchun,[b] Maksim S. Mikhailov,[d] Pavel A. Stuzhin,[d] Akihiro Otsuka,[c] Hideki Yamochi,[c] Gunzi Saito,*[e,f] and Rimma N. Lyubovskaya[a]

Abstract: Oxidation of {cryptand(Na^+)}($C_{60}^{\bullet-}$) and {cryptand(Na^+)}$_2$(C_{60}^{2-}) with integer −1 and −2 charges on fullerene by iron(II) octaethyltetrapyrazinoporphyrazine allows crystallization of complexes with noninteger average charge on C_{60}. {Cryptand(Na^+)}(C_{60})$_3^-$·2$C_6H_4Cl_2$ (**1**) with partial −0.33 charge on C_{60} has closely packed 3D structure formed by fragments of hexagonal fullerene layers. Complex **1** shows high conductivity of 50-60 and 100-250 $S\cdot cm^{-1}$ in the 295-120 K range measured by four-probe and microwave techniques, respectively. Metallic behavior of **1** is observed down to 150-120 K. It manifests a broad band in the IR range

with maximum at 2000 cm^{-1} attributed to the intraband transition in metal and a Dysonian EPR signal characteristic of highly conducting materials. Metallic conductivity is still observed in **1** after one month exposure to air. {Cryptand(Na^+)}(C_{60})$_2^-$ (**2**) and {cryptand(Na^+)}$_8$(C_{60})$_6^{8-}$ (**3**) with average −0.5 and −1.33 charges on C_{60} do not show metallic conductivity. This

Keywords: fullerene, complexes with partial charge transfer, metallic conductivity, charge disproportionation, crystal structure, IR and UV-visible-NIR spectra, magnetic properties

can be explained by charge disproportionation and the formation of neutral and −1 charged C_{60} in **2** due to their different cationic surrounding. Complex **3** has highly symmetric cationic surrounding for C_{60}. Nevertheless, charge disproportionation also realized in **3** provides −1 and −2 charged C_{60}. No dimerization of C_{60} is observed in **1** and **2** in spite of close packing of fullerenes in crystals. On the contrary, diamagnetic singly bonded (C_{60}^-)$_2$ dimers are formed in {cryptand(Li^+)}$_2$(C_{60}^-)$_2$·$C_6H_4Cl_2$·C_6H_{14} (**4**) with full −1 charge on fullerene as usually observed for the $C_{60}^{\bullet-}$ salts with close fullerene packing.

Introduction

Fullerenes can show promising conducting properties.[1-7] Till now conducting fullerene compounds have been obtained mainly by fullerene doping with alkali, alkali-earth and lanthanide metals.[1-4]

[a] Dr. D.V. Konarev, Dr. E. I. Yudanova, Prof. R. N. Lyubovskaya,
Institute
 of Problems of Chemical Physics RAS, Chernogolovka, Moscow
region,
 142432 (Russia), E-mail: konarev@icp.ac.ru

[b] Dr. S.S. Khasanov, Dr. A.F. Shevchun
 Institute of Solid State Physics RAS, Chernogolovka, Moscow
region, 142432 (Russia)

[c] Dr. A. Otsuka, Dr. M. Ishikawa, Prof. H. Yamochi
 Research Center for Low Temperature and Materials Sciences,
Kyoto University, Sakyo-ku, Kyoto 606-8501 (Japan)

[d] Dr. M. S. Mikhailov, Prof. P. A. Stuzhin,
 Research Institute of Macroheterocycles, Ivanovo State University of
Chemistry and Technology, Ivanovo, 153000 (Russia)

[e] Prof. Dr. Gunzi Saito
 Faculty of Agriculture, Meijo University, 1-501 Shiogamaguchi,
Tempaku-
 ku, Nagoya 468-8502 (Japan), E-mail: gsaito@ccmfs.meijo-u.ac.jp

[f] Toyota Physical and Chemical Research Institute, 41-1, Yokomichi,
 Nagakute, Aichi 480-1192 (Japan)

The (M^+)($C_{60}^{\bullet-}$) salts contain one-dimensional metallic polymers,[4] while salts of the (M^+)$_3$(C_{60}^{3-}) (M = K, Rb and Cs) composition with three-dimensional (3D) packing of fullerenes are metals, which transmit to the superconducting state below 38 K under pressure and 33 K in ambient conditions.[1-3] Being prepared by doping in gas phase these salts are generally obtained as powders. Conducting fullerene compounds can be obtained as crystals by direct growth from solution. Quasi-two-dimensional metallic conductivity is observed in the (MDABCO$^+$)($C_{60}^{\bullet-}$)·TPC salt (where MDABCO$^+$ is *N*-methyldiazabicyclooctanium cation, TPC is triptycene) containing closely packed hexagonal fullerene layers.[5, 6] In spite of layered structure, (K^+)(THF)$_5$($C_{60}^{\bullet-}$)·2THF shows one-dimensional electric conductivity.[7] All these compounds manifest integer charge transfer (CT) to the fullerene molecule, namely, −1, −2, −3, etc.

In contrast to fullerenes, conducting compounds based on oxidized substituted tetrachalcogenofulvalenes[8] and metal phthalocyanines[9] as well as reduced 7,7,8,8-tetracyanoquinodimethanes[10] and M(dmit)$_2$ (M = Ni, Pd, Pt, dmit is 1,3-dithiol-2-thione-4,5-dithiolate)[11] have mainly partial and noninteger CT to donor or acceptor molecules (for example, charge transfer degree is δ = 0.5 or 0.67). Combined with appropriate crystal structures, partial CT provides metallic conductivity by forming a partially filled conduction band. At full CT, Coulomb repulsion between electrons begins to play an important role to localize electrons and form insulating magnetic states. Therefore,

compounds with partial CT to the fullerene molecule in conjunction with the presence of degenerated frontier molecular orbitals can be promising candidates to develop highly conducting systems. Though many ionic compounds based on fullerenes are known, only several compounds with partial and noninteger CT have been obtained. $(Na^+)_x(THF)_yC_{60}$ (x ~ 0.4, y ~ 2.2)[12] shows conductivity of 50 $S\cdot cm^{-1}$ at room temperature (RT) and metallic behavior which can be explained by partial CT ($\delta \sim -0.4$). The phase transition at 170 K results in the insulating state. Similar compounds were obtained with K^+ and Li^+ cations.[13] The latter compound shows high conductivity (30 $S\cdot cm^{-1}$ at RT) but semiconducting behavior. Unfortunately, exact crystal structures of these compounds are unknown. Another fullerene complex with noninteger average charge on C_{60} is $\{(Ph_3P)_3Au^+\}_2(C_{60})_3^{2-}\cdot C_6H_4Cl_2$. It contains corrugated hexagonal fullerene layers and has two $(Ph_3P)_3Au^+$ cations per three C_{60} molecules. Average charge on C_{60} is -0.67. Charges on the fullerene molecules were estimated to be -1 for two of C_{60} and close to zero for one of C_{60}. Differently charged fullerenes have different cationic surroundings since positively charged gold atoms of $(Ph_3P)_3Au^+$ approach closer to $C_{60}^{\bullet-}$. Charge disproportionation provides no metallic conductivity.[14] Two other complexes with noninteger average charge on C_{60} are $\{(DMETEP^+)\cdot Zn^{II}OEP\}(C_{60})_{1.5}^{-}\cdot C_6H_4Cl_2$ (OEP is octaethyl-porphyrin; $DMETEP^+$ is N,N'-dimethyl-N-ethylthioethylpiperazini-um cation)[15] and $\{DB18C6(K^+)\}_4(C_{60})_5^{4-}\cdot 12THF$ (DB18C6 is dibenzo-18-crown-6-ether).[16] Negatively charged and neutral fullerenes are spatially separated in these complexes, and charge disproportionation is also caused most probably by different cationic surroundings of C_{60}.

In this work we report on the new general strategy developed for preparation of fullerene complexes with noninteger average CT to fullerene using iron(II) octaethyltetrapyrazinoporphyrazine ($Fe^{II}TPyzPzEt_8$) as oxidizer for fullerene salts. Crystallization of $\{cryptand(Na^+)\}(C_{60}^{\bullet-})$ and $\{cryptand(Na^+)\}_2(C_{60}^{2-})$ in the presence of $Fe^{II}TPyzPzEt_8$ yields complexes: $\{cryptand(Na^+)\}(C_{60})_3^{-}\cdot 2C_6H_4Cl_2$ (**1**), $\{cryptand(Na^+)\}(C_{60})_2^{-}$ (**2**) and $\{cryptand(Na^+)\}_8(C_{60})_6^{8-}$ (**3**) with average -0.33, -0.5 and -1.33 charges on C_{60}, respectively (cryptand is 4,7,13,16,21,24-hexaoxa-1,10-diazabicyclo[8.8.8]hexacosane). Complex **1** is metal, whereas complexes **2** and **3** are non-metals and show charge disproportionation. Complexes **1** and **2** are air-stable and dimerization of fullerenes is not realized in them in spite of their close 3D packing. $\{Cryptand(Li^+)\}_2(C_{60}^{-})_2\cdot C_6H_4Cl_2\cdot C_6H_{14}$ (**4**) has full -1 charge on fullerene and in this case singly bonded $(C_{60}^{-})_2$ dimers are formed. We present and discuss optical, magnetic and conducting properties of **1-4**.

Results and Discussion

1 Synthesis

The choice of mild oxidizer is crucial for the synthesis of C_{60} complexes with noninteger average CT to fullerene. The first and second reduction potentials for C_{60} are -0.45 and -0.82 V vs SCE in non-coordinating o-dichlorobenzene[17]. Therefore, negative reduction potential for appropriate oxidizer should be lower. In this work iron(II) octaethyltetrapyrazinoporphyrazine ($Fe^{II}TPyzPzEt_8$)

was found to be suitable oxidizer for fullerene anions. The 1st well-defined reduction wave observed for $Fe^{II}TPyzPzEt_8$ in coordinating DMSO at -0.19 V (vs Ag/AgCl) (Figure S1) or -0.235 V (vs SCE) can be assigned to the Fe^{II}/Fe^{I} reduction couple with the formation of the $[Fe^{I}TPyzPzEt_8(2-)]^-$ anion. As a result, $Fe^{II}TPyzPzEt_8$ shows stronger acceptor properties than C_{60} and can partially oxidize the $\{cryptand(Na^+)\}(C_{60}^{\bullet-})$ or $\{cryptand(Na^+)\}_2(C_{60}^{2-})$ salts whereas $Fe^{II}TPyzPzEt_8$ is dissolved to form deep violet $\{cryptand(Na^+)\}\{Fe^{I}TPyzPzEt_8(2-)\}^-$ salt. Dissolution of stoichiometric amount of $Fe^{II}TPyzPzEt_8$ together with $\{cryptand(Na^+)\}(C_{60}^{\bullet-})$ followed by precipitation of crystals by hexane allow **1** and **2** to be crystallized together with the $\{cryptand(Na^+)\}(C_{60}^{\bullet-})\cdot C_6H_4Cl_2$ salt with full -1 charge on C_{60}. Dissolution of stoichiometric amount of $Fe^{II}TPyzPzEt_8$ together with $\{cryptand(Na^+)\}_2(C_{60}^{2-})$ followed by precipitation of crystals by hexane allow the crystals of **3** to be obtained together with the crystals of $\{cryptand(Na^+)\}(C_{60}^{\bullet-})\cdot C_6H_4Cl_2$ and $\{cryptand(Na^+)\}_2(C_{60}^{2-})$[18]. Single crystal samples of fullerene complexes obtained in both syntheses have been identified by X-ray diffraction. The crystal samples of different phases are separated easily due to their shape (crystal habit). All the measurements of optical, EPR spectra and conductivity of **1-3** were carried out on the single crystal samples, one or several ones, separated under microscope in accordance of their habit and tested by X-ray diffraction, i.e. well identified crystal samples. We also suppose that complexes with noninteger average CT to C_{60} could be obtained by adding corresponding amount of neutral C_{60} to the solutions of $\{cryptand(Na^+)\}(C_{60}^{\bullet-})$ or $\{cryptand(Na^+)\}_2(C_{60}^{2-})$. However, no crystals of the complexes with noninteger CT to C_{60} were obtained in this case.

2 Crystal structure, optical, magnetic and conducting properties of $\{cryptand(Na^+)\}(C_{60})_3^{-}\cdot 2C_6H_4Cl_2$ (**1**)

Crystal structure of **1** was determined from X-ray diffraction on a single crystal. In spite of slow cooling down to 90 K, all components of the complex are strongly disordered (see Experimental part). We show only major orientation for the disordered parts in Fig. 1. There are three fullerenes per one cryptand(Na^+) cation. Average charge on C_{60} is -0.33, and **1** is a complex with noninteger CT to fullerene.

Complex **1** has close 3D packing of fullerenes penetrated by continuous channels occupied by the cryptand(Na^+) cations and solvent $C_6H_4Cl_2$ molecules located in the corners of each channel (Fig. 1a). The fragments of nearly ideal hexagonal fullerene layers are located in the plane approximately parallel to the diagonal to the ac plane and the b axis (Fig. 1b). These fragments have width of three fullerene rows since they are separated by the channels (Fig. 1b). As a result, fullerenes from the central row have six fullerene neighbors, and each C_{60} from the rows adjacent to the channels has only four fullerene neighbors. All interfullerene center-to-center (ctc) distances in these fragments are in the 9.85-9.95 Å range (Fig. 1b). Hexagonal fullerene fragments are also closely packed along the c axis with the ctc interfullerene distance of only 9.95 Å (Fig. 1a). All these distances are essentially shorter than the van der Waals (vdW) diameter of C_{60} of 10.18 Å. Potentially electron conductivity can be realized approximately along the plane parallel to the diagonal to the ac plane and the b axis.

To discuss the possibility of charge disproportionation in **1** the conditions for electrostatic interaction between the cryptand(Na$^+$) cations and fullerenes should be considered. Each of three independent fullerenes in **1** is surrounded by three cations. The shortest distances between the centers of three independent C$_{60}$ and the Na$^+$ ions are close (8.12, 8.16 and 8.18 Å). Other cations have essentially longer distances between the centers of C$_{60}$ and the Na$^+$ ions which are also rather close for three independent C$_{60}$ (10.05-10.32 Å). Therefore, conditions for electrostatic interactions of three independent fullerenes with the cations are similar and that can provide delocalization of negative charge over fullerenes.

Conductivity of **1** was measured by four-probe and microwave techniques on oriented single crystals from advanced crystal surface parallel to the crystallographic (101) plane (the plane coming along the *b* axis and the diagonal to the *ac* plane as shown in inset in Fig. 2a). High RT conductivity of the crystal of 55 S·cm^{-1} increases with the temperature decrease down to 220 K showing metallic behavior. Conductivity decreases slightly below this temperature and the abrupt decrease of conductivity is observed only below 120 K showing the transition to the semiconducting state (E_a estimated at $T < 30$ K is about 6 meV).

Microwave conductivity was also measured for oriented single crystal in the same plane. The frequency dependence of surface impedance calculated from microwave absorption in the $120 < T < 200$ K range corresponds to the normal skin effect in the compound with free carriers. Microwave conductivity of 100-240 S·cm^{-1} in the 120-200 K range (Fig. 2b) is higher than conductivity measured by four-probe technique and shows metallic behavior down to 120 K. Transition to the nonmetallic state is observed below 120 K since absorption at $T = 5$ K and the frequency dependence of microwave absorption are absent in the 120-5 K range.

The UV-visible-NIR and IR spectra of **1** are shown in Fig. 3. Bands with the maxima at 346 and 1072 nm (Fig. 3a, arrows) were attributed to fullerenes. The latter band is generally ascribed to C$_{60}^{\bullet-}$. A broad weak band at 667 nm (Fig. 3a, arrow) can most probably be attributed to CT between neutral fullerenes. It is known that the CT band associated with electron transfer between fullerenes is manifested in the spectrum of C$_{60}$ at about 450 nm[19]. The lowest energy absorption band can be found even in the IR range with the maximum at about 2000 cm^{-1} (Fig. 3b). The origin of this band can be interpreted by either an intraband transition in metal or intermolecular CT from D^0 (or A$^{\bullet-}$) to D$^{\bullet+}$ (or A^0) for the charge separated case. Only in a rare system with extremely small on-site Coulomb repulsion, a low-energy band appears from the CT process between D$^{\bullet+}$ (or A$^{\bullet-}$) ions. The energy of the CT process between cryptand(Na$^+$) and C$_{60}$ should be high whereas CT between C$_{60}^{\bullet-}$ is not observed at such low energies. Generally, bands associated with

CT between C$_{60}^{\bullet-}$ are manifested in the spectra of the salts at wavenumbers higher than 5500 cm^{-1} [6]. Thus, the band at 2000 cm^{-1} can be attributed to the intraband transition in metal or CT between C$_{60}^0$ and C$_{60}^{\bullet-}$ and that well agrees with metallic conductivity in this compound at RT. The F_{1u}(4) C$_{60}$ mode which is sensitive to CT to the fullerene molecule is not well defined and manifested at about 1403 cm^{-1} (Table S1), that is intermediate position between those characteristic of C$_{60}^0$ and C$_{60}^{\bullet-}$.

The electron paramagnetic resonance (EPR) spectra of single crystals with microwave electric field directed parallel to the (101)
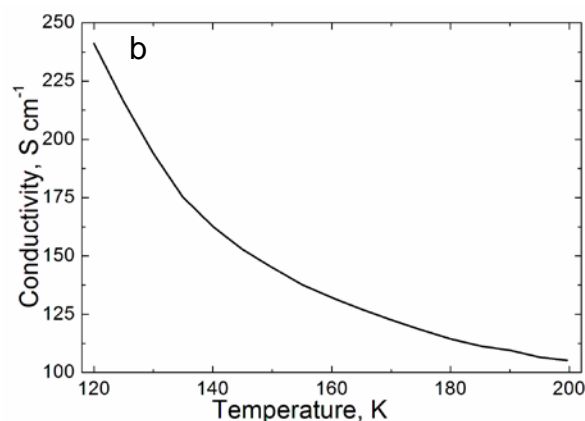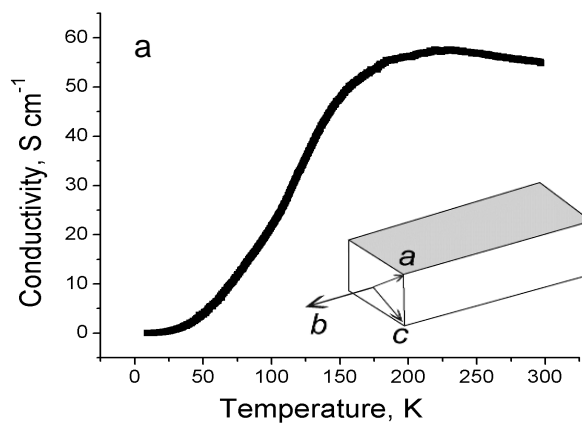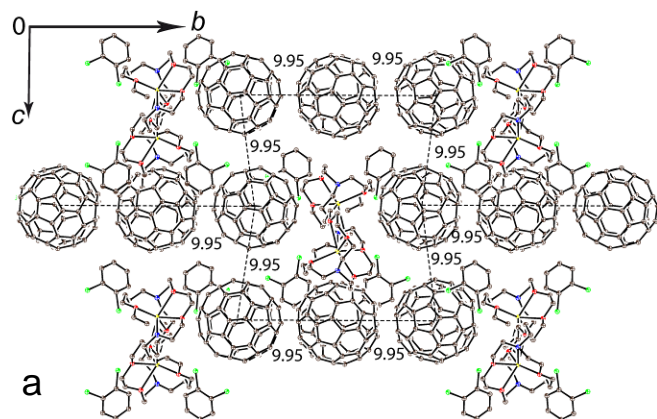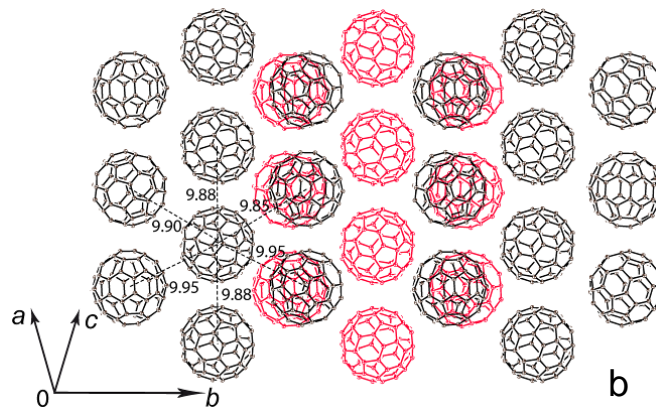

Figure 2. (a) Conductivity of oriented single crystal of **1** measured by four-probe technique in anaerobic conditions; (b) microwave conductivity measured in the 200-120 K range. Inset shows the directions of crystallographic axes in a crystal, advanced crystal surface from which both conductivities were measured is shown by grey color.

Figure 1. (a) View on crystal structure of {cryptand(Na$^+$)}(C$_{60}$)$_3$$^{-}$·2C$_6H_4Cl_2$ (**1**) along the *a* axis; (b) view on fragments of hexagonal fullerene layers (fragments located at $z = 0.5$ and 1 are drawn in black and red, respectively). Fullerenes, cations and solvent molecules are shown in major orientation.
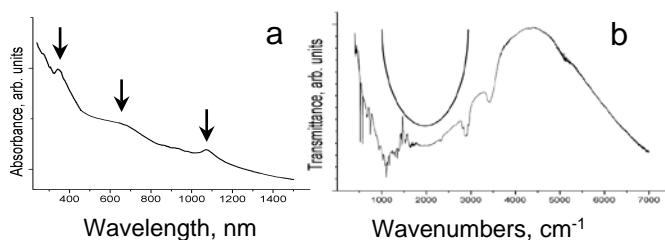
Figure 3. UV-visible-NIR (a) and IR spectra (b) of **1** measured in KBr pellets prepared in anaerobic conditions.

plane showed the signal with g = 1.9966 and a linewidth (ΔH) of 3.0 mT (RT) ascribed to $C_{60}^{\bullet-}$. The signal has an asymmetric Dysonian shape characteristic of highly conductive materials (Fig. 4, inset). Such EPR signals were observed in quasi-2D organic metals and superconductors based on bis(ethylenedithio)tetrathiafulvalene (ET), e.g. $[\beta–(ET)_2I_3]$[20] and fullerene, e.g. $(MDABCO^+)(C_{60}^{\bullet-})\cdot TPC$[5]. The asymmetry ratio between the maximum and the minimum of the absorption derivative (A/B) depends on crystal and varies from 1.8 to 2.6 at RT. A/B exhibits a gradual increase from 310 down to 180 K and decreases below this temperature. The abrupt decrease of A/B is observed below 120 K (Fig. 4). Such behavior corresponds well to the temperature dependence of conductivity measured by four-probe technique. It is interesting that the EPR signal from the single crystal with microwave electric field directed parallel to the (010) plane shows a shape close to the Lorentzian one. Therefore, the Dysonian shape of the EPR signal is due to a skin effect. In spite of 3D packing of fullerenes in **1**, conductivity is anisotropic and that in the $(10\bar{1})$ is higher than that in the (010) plane. Integral intensity of the almost Lorentzian shaped signal showed a nearly temperature independent behavior down to 120 K as it should be observed for the metals showing temperature independent Pauli paramagnetism[5]. G-factor of the EPR signal is nearly temperature independent in metallic state and increases noticeably at the transition of the complex to the semiconducting state below 120 K (Fig. 4). The EPR signal linewidth decreases with temperature as in other $C_{60}^{\bullet-}$ salts. Slight broadening of the EPR signal below 20 K can be due to weak magnetic coupling of spins manifested at low temperatures.
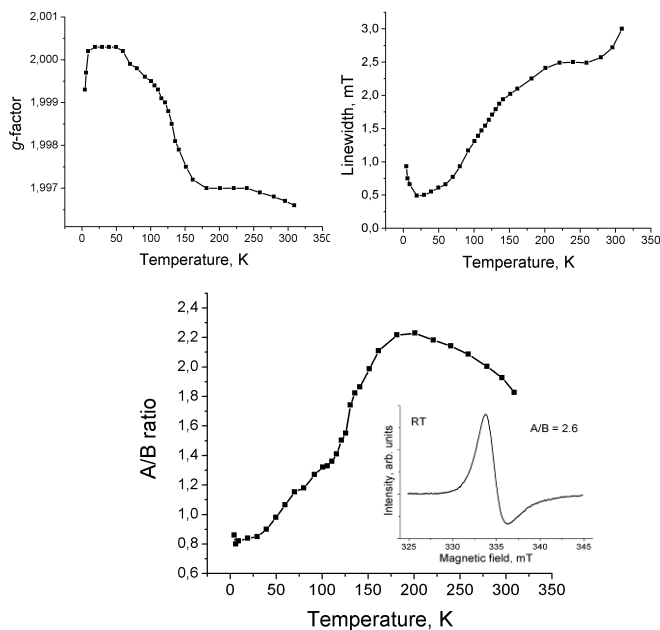

Figure 4. Temperature dependence of g-factor, linewidth and the A/B ratio for a single crystal of **1**. Inset shows Dysonian type EPR signal of **1** at room temperature (RT).
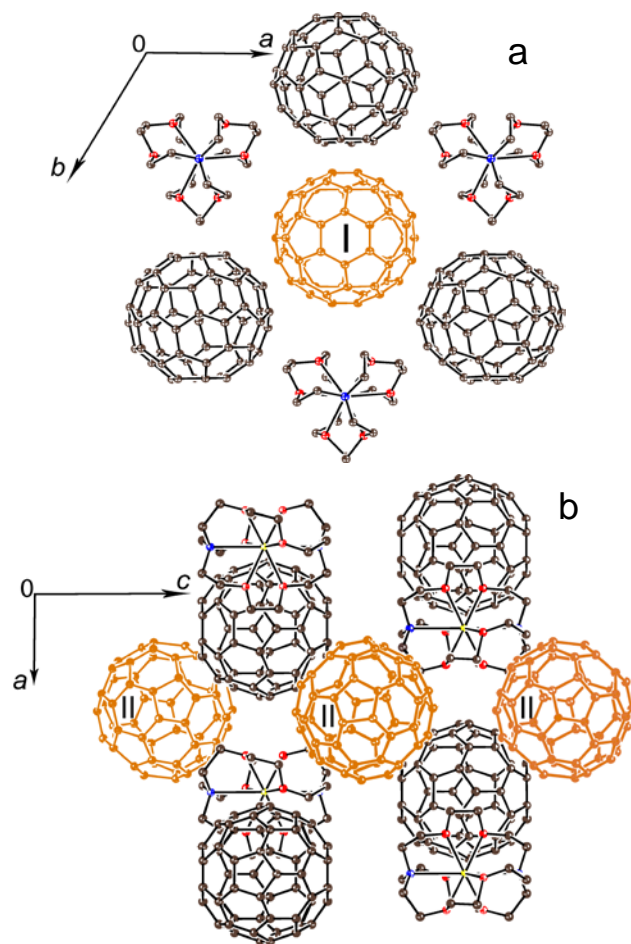

Figure 5. Surrounding of two independent fullerenes of types I and II in **2**. Only one orientation is shown for the fullerenes and the cryptand(Na$^+$) cations.

Exposure of single crystal of **1** to air during one month does not change the Dysonian shape of the EPR signal. Therefore, this complex is air stable and metallic conductivity is not affected by air oxidation.

3 Crystal structure and optical properties of {cryptand(Na$^+$)}(C$_{60}$)$_2^-$ (2)

Compound **2** was obtained as well-shaped large hexagonal plates. The structure of **2** was determined from X-ray diffraction on single crystal. There are two independent C_{60} of type I and II (Fig. 5) per one cryptand(Na$^+$) cation in **2** indicating the formation of a complex with –0.5 charge on fullerene as average.

The complex has hexagonal 3D packing of fullerenes in a crystal with short interfullerene ctc distances. Fullerenes of type I (Fig. 5a) are located in the center of a trihedral prism composed of six fullerenes with ctc distances of 9.86 (three neighbors located above fullerene) and 9.93 Å (three neighbors located below fullerene). Fullerenes of type II (Fig. 5b) are located in the center of a distorted prism from six fullerene neighbors. In this case the ctc interfullerene distances are 9.93-9.96 Å. Fullerene of type I (Fig. 5a) is surrounded by three cryptand(Na$^+$) cations with a short distance between the center of C_{60} and the Na$^+$ ions of only 8.446 Å. Fullerene of type II (Fig. 5b) is surrounded by four cations, and the distances between the center of C_{60} and the Na$^+$ ions are essentially longer (9.89-9.91 Å). These data show that conditions for electrostatic interaction between two independent fullerenes and the cryptand(Na$^+$) cations are different, and that can result in charge disproportionation in the fullerene framework accompanied by the

formation of −1 charged (fullerene of type I) and neutral C_{60} (fullerene of type II).

Indeed, the IR spectrum of **2** supports charge disproportionation due to the presence of the absorption bands of the $F_{1u}(4)$ C_{60} mode which is sensitive to CT to the fullerene molecule at 1390 and 1429 cm^{-1} (see Supporting information, Fig. S2). These positions correspond to the presence of −1 and neutral C_{60} in **2** [21, 22]. The bands in the spectrum of **2** in the UV-visible-NIR range at 264, 346 nm were attributed to neutral fullerene whereas the bands at 940 and 1080 nm were ascribed to $C_{60}^{\bullet-}$ (Fig. S5). A weak band in the visible range at 500 nm can be due to CT between fullerenes in **2**. A low-energy band in the IR range at about 2000 cm^{-1} is not observed in the spectrum of **2**.

Microwave conductivity was measured on single crystal of **2** in the 200-5 K range. The single crystal was oriented in such a way that current flew in the *ab* plane. Since absorption as well as the frequency dependence of microwave absorption were not found in the whole studied temperature range, it can be concluded that the crystal is not metallic that agrees with charge disproportionation which should suppress metallic conductivity.

4 Crystal structure, optical and magnetic properties of {cryptand(Na$^+$)}$_8$(C$_{60}$)$_6$$^{8-}$ (3)

Complex **3** has a highly symmetric trigonal unit cell with equal parameters $a = b = c = 20.1117(5)$ Å. There are two independent cryptand(Na$^+$) cations: one with full occupancy and the other one located on the 3-fold symmetry axis has 0.33 occupancy. There is also one independent fullerene C_{60} in **3** with full occupancy. As a result, complex **3** has 8 cations per 6 fullerene molecules and average charge on C_{60} is −1.33.

This complex shows close 3D packing which can be presented by alternation of the layers of two types along the *a* axis (Fig. 6). The layers are arranged in such a way that fullerenes from one layer are positioned exactly over the fullerenes from the adjacent layers. VdW C···C contacts between fullerenes are formed in the layers and with fullerenes from the adjacent layers located above and below the layer.

Each fullerene in the crystal structure of **3** is surrounded by four fullerene neighbors to form square environment. All four interfullerene ctc distances are equal to 10.056 Å (half of the unit cell parameter) and multiple short vdW C···C contacts are formed between them. Each fullerene has highly symmetric cationic
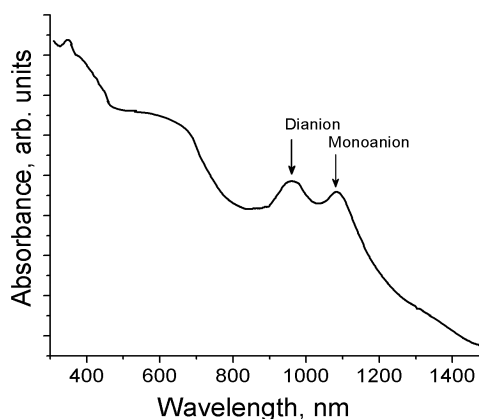

Figure 7. The UV-visible-NIR spectrum of **3** in KBr pellet prepared in anaerobic conditions.

surrounding from eight cryptand(Na$^+$) cations in **3**. In contrast to **2**, uniform cationic surrounding does not support charge disproportionation in **3**.

The UV-visible-NIR and IR spectra of **3** are shown in Figs. 7 and S3, respectively. Two bands in the NIR range with maxima at 960 and 1080 nm indicate the presence of −2 and −1 charged fullerenes (Fig. 7). An intense broad band at 660 nm (Fig. 7) appears most probably due to CT between fullerenes. It is known that the position of $F_{1u}(4)$ C_{60} mode is most sensitive to CT to a fullerene molecule and shifts from 1429 cm^{-1} (neutral C_{60}) to 1386-1396 and 1374-1377 cm^{-1} at the formation of −1 and −2 charged C_{60} [18, 21- 25]. The position of this mode in the IR spectrum of **3** at 1385 and about 1377 cm^{-1} corresponds to the presence of mono- and dianions of C_{60}. Thus, optical spectra support charge disproportionation in **3**.

To comprehend the magnetic properties of **3** magnetic behavior of individual mono- and dianions of C_{60} should be considered. Generally, monoanions of C_{60} show broad EPR signals at RT with *g*-factor = 1.996-2.000 and linewidth ΔH = 3-6 mT. The signals strongly narrow with decreasing temperature.[24-27] Dianions of C_{60} have temperature activated excited triplet state. They show a weak narrow signal below 150 K, and new broad signals with *g*-factor = 2.0004-2.0030 and ΔH = 2.76-5.60 mT appear above 150-170 K and their intensity grows with temperature [18, 24]. The EPR signal of **3** is strongly asymmetric in the 295-4 K range and can be fitted by three Lorentzian lines as shown in Fig. 8. The temperature dependence of
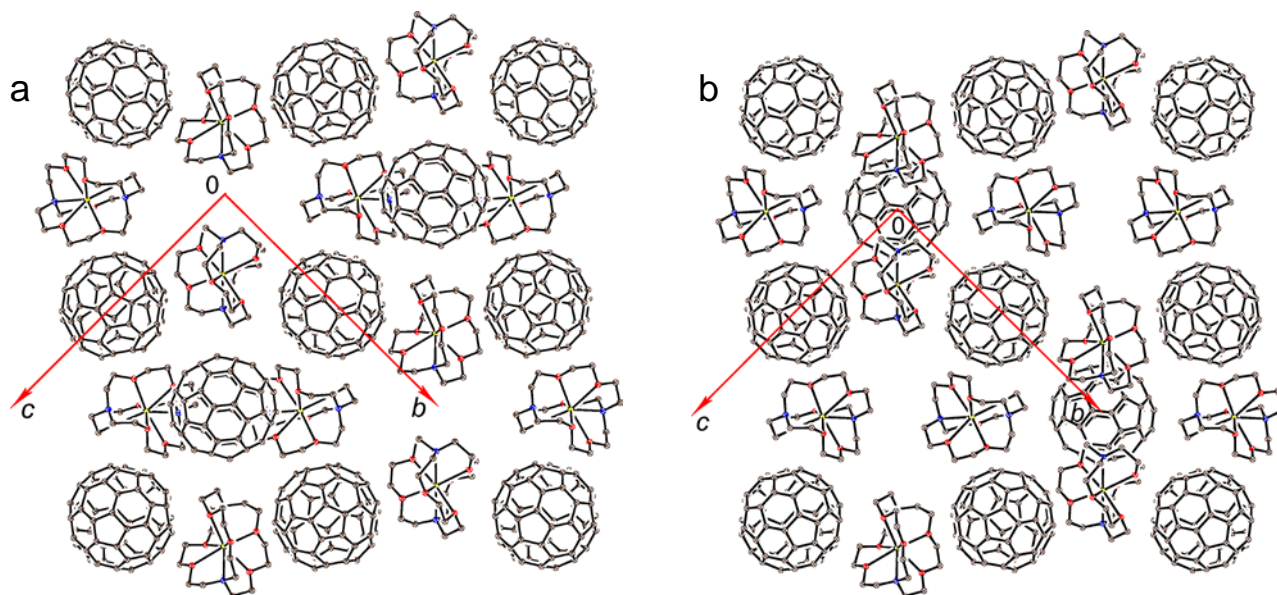

Figure 6. View along the *a* axis on two adjacent fullerene layers located at *a* = 0 (a) and 0.5 (b). These layers separated by cationic cryptand(Na$^+$) layer are located one after another along the *a* axis and form 3D fullerene packing in **3**.
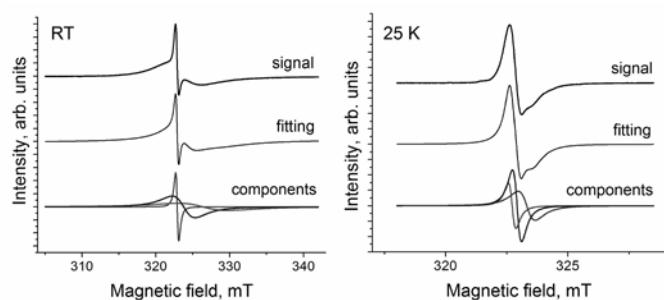
Figure 8. Fitting of EPR signal of polycrystalline **3** at RT and 25 K by three Lorentzian lines.

total integral intensity of three lines is shown in Fig. 9c. According to Fig. 9c there are two temperature ranges with different behavior. Integral intensity shows a pure paramagnetic dependence increasing with decreasing temperature in the 4-166 K range. Such behavior can be due to the presence of paramagnetic $C_{60}^{\bullet-}$ and the C_{60}^{-2} dianions with diamagnetic singlet ground state. In this temperature range, the signal can be fitted by three lines with $g_1 = 2.0017$ and ΔH of 0.37 mT, $g_2 = 1.9989$ and ΔH of 0.46 mT and $g_3 = 1.9967$ and ΔH of 1.78 mT (166 K). The narrow line is specified by temperature independent g-factor and linewidth. Similar narrow signals were found in the spectra of $C_{60}^{\bullet-}$ or C_{60}^{2-} [18, 23, 28, 29]. They can appear due to air oxidation of fullerene anions or the presence of impurities. The major two-component signal with g_2 and g_3 noticeably narrows with decreasing temperature and can be attributed to $C_{60}^{\bullet-}$. The parameters of the signal 25 K are $g_2 = 2.0007$ and ΔH of 0.37 mT and $g_3 = 1.9983$ and ΔH of 0.693 mT (Fig. 8). Integral intensity of the signal strongly grows above 166 K (Fig. 9c) most probably due to thermal population of the excited triplet state in the C_{60}^{-2} dianions. That is accompanied by the shift of g-factors of two components to lower values and their strong broadening (Figs. 9a and 9b). The RT parameters of these components are $g_2 = 1.9956$ and ΔH of 3.10 mT and $g_3 = 1.9800$ and ΔH of 6.74 mT. The EPR spectra together with the optical spectra indicate the presence of $C_{60}^{\bullet-}$ and C_{60}^{2-} in **3** most probably due to charge disproportionation.

Thus, in spite of similar cationic surrounding differently charged fullerenes with −1 and −2 charges are formed in **3**. We suppose that mono- and dianions are positionally disordered in a crystal. Therefore, they cannot be resolved by X-ray diffraction and the given C_{60} molecule is the average one.
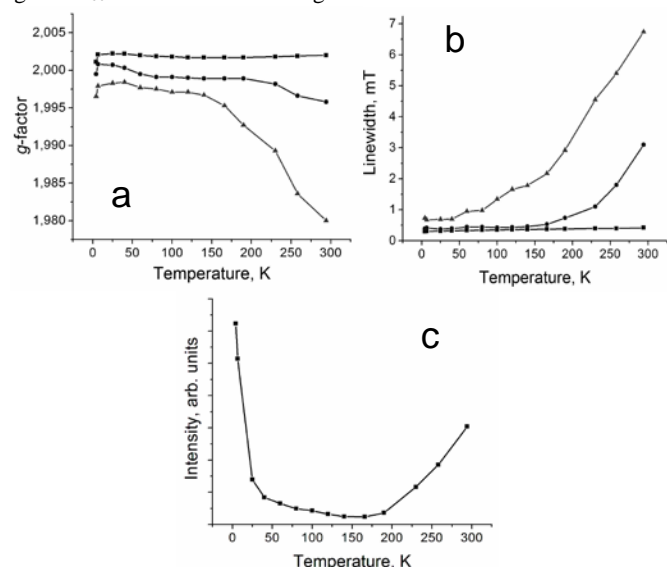

Figure 9. Temperature dependence of g-factor (a), linewidth (b) and integral intensity of three components (c) for polycrystalline **3**

5 Crystal structure and optical properties of {cryptand(Li⁺)}₂(C₆₀⁻)₂·C₆H₄Cl₂·C₆H₁₄ (4)

Complex **4** was obtained with the cryptand(Li⁺) counter cations without addition of $Fe^{II}TPyzPzEt_8$. The crystal structure determined at 120 K showed the presence of two cryptand(Li⁺) cations per two fullerene units and this salt has full −1 charge on fullerene. X-ray diffraction data also show that the $C_{60}^{\bullet-}$ radical anions are dimerized forming singly bonded $(C_{60}^-)_2$ dimers. The intercage C-C bond length is 1.602(8) and the interfullerene ctc distance is 9.3 Å as in other singly bonded $(C_{60}^-)_2$ dimers [16, 29-34]. The crystal structure of monomeric high-temperature phase of **4** cannot be solved due to disorder.

The optical spectrum of **4** corresponds to the presence of the $C_{60}^{\bullet-}$ radical anions due to that $F_{1u}(4)$ C_{60} mode appears as a single band at 1390 cm⁻¹ and intense bands of $C_{60}^{\bullet-}$ are manifested in the NIR range at 935 and 1072 nm (Figs. S4 and S6, respectively).

The salt manifests an intense EPR signal which can be fitted by narrow and broad components with $g_1 = 2.0002$ and ΔH of 0.51 mT and $g_2 = 1.9915$ and ΔH of 3.18 mT (RT). The broad component is ascribed to $C_{60}^{\bullet-}$. The broad component decreases strongly in intensity below 250 K due to dimerization of $C_{60}^{\bullet-}$ and the formation of diamagnetic and EPR silent singly bonded $(C_{60}^-)_2$ dimers. Previously, similar behavior was observed in many complexes and salts of $C_{60}^{\bullet-}$ with close fullerene packing[16, 29-34].

Dimerization of $C_{60}^{\bullet-}$, which most probably involves electrons from the singly occupied molecular orbital (SOMO) of $C_{60}^{\bullet-}$ results in the formation of a stable two-electron intercage C-C bond and the transition of the compounds from paramagnetic to the diamagnetic state. Since only one of two or three fullerene molecules has electron on SOMO of C_{60} in **1** and **2** with noninteger CT, no stable intercage C-C bonds are formed in this case and dimerization is not realized.
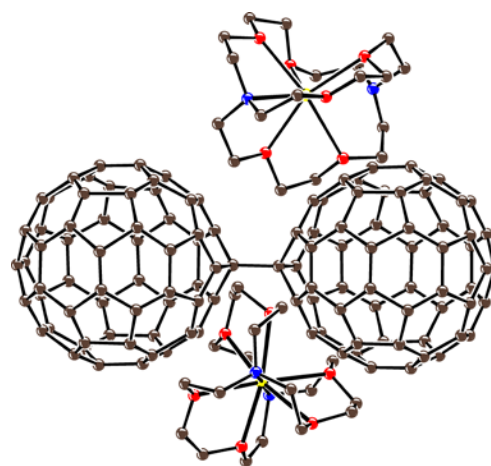

Figure 10. Crystal structure of dimeric phase of **4** at 120 K. Solvent molecules are not shown.

Conclusion

In this work we report on the new approach developed by us for the synthesis of crystalline fullerene complexes with noninteger average CT to the fullerene molecule ($\delta = -0.33$, -0.5 and -1.33) by oxidation of the salts with −1 and −2 charged fullerenes by iron(II) octaethyltetrapyrazinoporphyrazine. Depending of cationic surrounding, charges can be delocalized over fullerenes providing highly conducting metallic state in **1** or charge disproportionation is observed with the appearance of differently charged fullerenes in a crystal: neutral and −1 charged fullerenes in **2,** and −1 and −2

charged fullerenes in **3**. Complex **1** preserves metallic properties in the air allowing us to obtain air stable fullerene metal. We also found that no dimerization of fullerenes is observed in **1** and **2** though fullerenes are closely packed in crystals. Such peculiarities make fullerene complexes with noninteger CT to fullerene promising candidates to develop highly conducting air stable fullerene materials. Metallic state can realize in them at uniform cationic surrounding of fullerenes and the absence of charge disproportionation.

Acknowledgements

[1] A. F. Hebard, M. J. Rosseinsky, R. C. Haddon, D. W. Murphy, S. H. Glarum, T. T. M. Palstra, A. P. Ramirez, A. R. Kortan, *Nature* **1991**, *350*, 600-601.

[2] K. Tanigaki, K. Prassides, *J. Mater. Chem.* **1995**, *5*, 1515-1527

[3] A.Y. Ganin, Y. Takabayashi, P. Jeglič, D. Arčon, A. Potocnik, P.J. Baker, Y. Ohishi, M. T. McDonald, M.D. Tzirakis, A. McLennan, G.R. Darling, M. Takata, M.J. Rosseinsky, K. Prassides, *Nature* **2010**, *466*, 221-225.

[4] F. Bommeli, L. Degiorgi, D. Wachter, Ö. Legeza, A. Jánossy, G. Oszlanyi, O. Chauvet, L. Forro, *Phys. Rev. B* **1995**, *51*, 14794-14797.

[5] D. V. Konarev, S. S. Khasanov, A. Otsuka, M. Maesato, G. Saito, R. N. Lyubovskaya, *Angew. Chem. Int. Ed.* **2010**, *49*, 4829-4832.

[6] D. V. Konarev, S. S. Khasanov, A. Otsuka, M. Maesato, M. Uruichi, K. Yakushi, A. Shevchun, H. Yamochi, G. Saito, R. N. Lyubovskaya, *Chem. Eur. J.* **2014**, *20*, 7268–7277.

[7] A. Kromer, U. Wedig, E. Roduner, M. Jansen, K. Yu. Amsharov, *Angew. Chem. Int. Ed.* **2013**, *52*, 12610–12614.

[8] a) J. M. Williams, J. R. Ferraro, R. J. Thorn, K. D. Carlson, U. Geiser, H. H. Wang, A.M. Kini, M.- H. Whangbo. *Organic Superconductors (including Fullerenes). Synthesis, Structure, Properties and Theory*, Prentice Hall, New Jersey: Englewood Cliffs, 1992; b) T. Ishiguro, G. Saito, K. Yamaji, *Organic Superconductors* 2-nd edn., Springer Ser. In Solid-State Sci. Vol. 51. Berlin, Heidelberg, New York, **1998**, pp. 1-522; c) G. Saito, Y. Yoshida, *Chem. Record* **2011**, *11*, 124-145

[9] T. Inabe, H. Tajima, *Chem. Rev.* **2004**, *104*, 5503-5534.

[10] a) I.F. Shchegolev, *Phys. Status Solidi A*, **1972**, *12*, 9-45; J. S. Pedersen, K. Carneiro, *Rep. Prog. Phys.* **1987**, *50*, 995-1043.

[11] P. Cassoux, L. Valade, H. Kobaayashi, A. Kobayashi, R.A. Clark, A.E. Underhill, *Coord. Chem. Rev*. **1991**, *110*, 115-160.

[12] H. Kobayashi, H. Tomita, H. Moriyama, A. Kobayashi, T. Watanabe, *J. Am. Chem. Soc*. **1994**, *116*, 3153-3154.

[13] a) H. Moriyama, H. Kobayashi, A. Kobayashi, T. Watanabe, *Chem. Phys. Lett*. **1995**, *238*, 116-121; b) H. Moriyama, M. Abe, H. Motoki, T. Watanabe, S. Hayashi, H. Kobayashi, *Synth. Met*. **1998**, *94*, 167-171.

[14] D. V. Konarev, S. S. Khasanov, A. Otsuka, H. Yamochi, G. Saito, R. N. Lyubovskaya, *Inorg. Chem.* **2014**, *53*, 6850−6855.

[15] D. V. Konarev, S. S. Khasanov, G. Saito, R. N. Lyubovskaya, *Cryst. Growth Des.* **2009**, *9*, 1170-1181.

[16] N. V. Kozhemyakina, K. Y. Amsharov, J. Nuss, M. Jansen, *Chem. Eur. J.* **2011**, *17*, 1798 – 1805.

[17] I. Noviandri, R. D. Bolskar, P. A. Lay, C. A. Reed, *J. Phys.Chem. B* **1997**, *101*, 6350-6358.

[18] D. V. Konarev, A. V. Kuzmin, S. V. Simonov, S. S. Khasanov, E. I. Yudanova, G. Saito, R. N. Lyubovskaya, *Phys. Chem. Chem. Phys.* **2013**, *15*, 9136-9144.

[19] H. J. Byrne, in Progress in Fullerene Research, Eds H. Kuzmany, J. Fink, M. Mehring, S. Roth, Singapore: World Scientific, 1995, p. 183-195.

[20] T. Sugano, G. Saito, M. Kinoshita, *Phys. Rev. B*. **1986**, *34*, 117-125.

[21] T. Picher, R. Winkler, H. Kuzmany, *Phys. Rev. B* **1994**, *49*, 15879 – 15889.

[22] V. N. Semkin, N. G. Spitsina, S. Krol, A. Graja, *Chem. Phys. Lett*. **1996**, *256*, 616-622.

[23] D. V. Konarev, S. S. Khasanov, G. Saito, I. I. Vorontsov, A. Otsuka, R. N. Lyubovskaya, Yu. M. Antipin, *Inorg. Chem*., **2003**, *42*, 3706-3708.

[24] D. V. Konarev, R. N. Lyubovskaya, *Russ. Chem. Rev*. **2012**, *81*, 336-366.

[25] C.A. Reed, R.D. Bolskar, *Chem. Rev*. **2000**, *100*, 1075-1120.

[26] A. Pènicaud, A. Peréz-Benítez, R. Gleason V., E. Muñoz P, R. Escudero, *J.Am.Chem.Soc*. **1993**, *115*, 10392-10393.

[27] D. V. Konarev, A. Yu. Kovalevsky, S. S. Khasanov, G. Saito, A. Otsuka, R. N. Lyubovskaya, *Eur. J. Inorg. Chem*., **2005**, 4822-4828.

[28] A. L. Litvinov, D. V. Konarev, E. I. Yudanova, M. G. Kaplunov, R. N. Lyubovskaya, *Russ. Chem. Bull*. **2002**, *51*, 2003-2007.

[29] D. V. Konarev, S. S. Khasanov, G. Saito, A. Otsuka, Y. Yoshida, R.N. Lyubovskaya *J. Am. Chem. Soc*. **2003**, *125*, 10074-10083.

[30] D. V. Konarev, S. S. Khasanov, A. Y. Kovalevsky, G. Saito, A. Otsuka, R. N. Lyubovskaya, *Dalton Trans.*, **2006**, 3716-3720.

[31] D. V. Konarev, S. S. Khasanov, A. Otsuka, G. Saito, R. N. Lyubovskaya. *Inorg. Chem.* **2007**, *46*, 2261-2271.

[32] E. A. Schupak, D. M. Lyubov, E. V. Baranov, G. K. Fukin, O. N. Suvorova, A. A. Trifonov, *Organomet.* **2010**, *29*, 6141–6144

[33] D. V. Konarev, S. S. Khasanov, G. Saito, A. Otsuka, R. N. Lyubovskaya, *J. Mater. Chem.* **2007**, *17*, 4171-4177.

[34] D. V. Konarev, S. S. Khasanov, R. N. Lyubovskaya, *Russ. Chem. Bull*. **2007**, *56*, 371-392.

Entry for the Table of Contents

Complexes {cryptand(M$^+$)} : (C$_{60}$) with full and partial charge transfer

1 : 3   1 : 2   1 : 1   8 : 6

A series of complexes with noninteger average charge on fullerene is obtained. {Cryptand(Na$^+$)}(C$_{60}$)$_3^-$·2C$_6$H$_4$Cl$_2$ (**1**) with partial −0.33 charge on C$_{60}$ shows metallic behavior down to 150-120 K which is preserved after one month exposure to air. {Cryptand(Na$^+$)}(C$_{60}$)$_2^-$ (**2**) and {cryptand(Na$^+$)}$_8$(C$_{60}$)$_6^{8-}$ (**3**) with average −0.5 and −1.33 charges on C$_{60}$ are nonmetals due to charge disproportionation. No dimerization of C$_{60}$ is observed in **1**-**2** in spite of close fullerene packing. The (C$_{60}^-$)$_2$ dimers are formed in {cryptand(Li$^+$)}$_2$(C$_{60}^-$)$_2$·C$_6$H$_4$Cl$_2$·C$_6$H$_{14}$ (**4**) with full −1 charge on C$_{60}$.

Supporting information

Electrochemistry for Fe^{II}TPyzPzEt$_8$
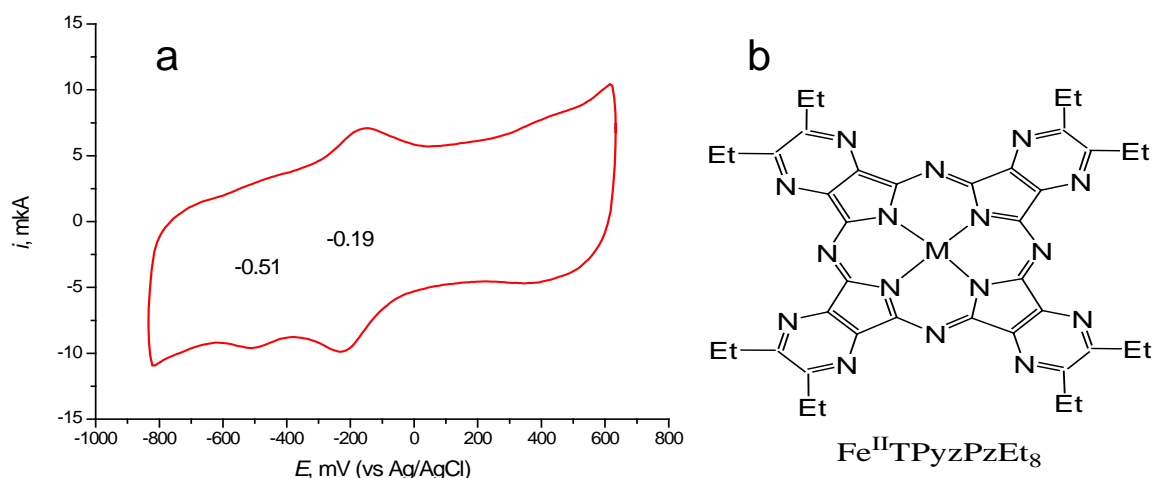
Figure S1. (a) Cyclic voltammogram of Fe^{II}TPyzPzEt$_8$ in DMSO containing 0.1 M TBAP; 100 mV/s potential scan rate. (b) Molecular structure of Fe^{II}TPyzPzEt$_8$.

Fe^{II}TPyzPzEt$_8$ undergoes two reduction processes in coordinating DMSO leading to monoanionic forms (Figure S1). The 1st well-defined reduction wave observed at E$^{1/2}$ = –0.19 V *vs* Ag/AgCl can be assigned to the Fe^{II}/Fe^{I} reduction couple and the formation of [Fe^{I}TPyzPz(2–)Et$_8$]$^{-}$. Less intense irreversible reduction observed at cathodic potential of –0.51 V *vs* Ag/AgCl (Figure S1) corresponds very likely to the reduction of the macrocycle and the formation of the [Fe^{II}TPyzPz(3–)Et$_8$]$^{\bullet-}$ radical anions since this value is similar to that of the 1st reduction potential for the complexes of alkyl substituted TPyzPzs with redox-inactive metals (–0.50 - –0.55 V [1,2]). The irreversibility of this process for Fe^{II}TPyzPzEt$_8$ and the absence of the corresponding anodic wave might be explained by valence isomerism of [Fe^{II}TPyzPz(3–)Et$_8$)]$^{\bullet-}$. The isomerisation in coordinating DMSO involves transfer from the hexacoordinated d^6 radical anion [Fe^{II}TPyzPzEt$_8$(3–)(DMSO)$_2$]$^{\bullet-}$ to more stable pentacoordinated d^7 anion [Fe^{I}TPyzPzEt$_8$(2–)(DMSO)]$^{-}$. The reversible formation of dianion is seen at –0.95 V *vs* Ag/AgCl, i.e. at potential value similar to that of the dianion of the Co^{I} complex [Co^{I}TPyzPzEt$_8$(3–)]$^{2-}$ [3] and π-dianions of alkyl substituted TPyzPzs with redox-inactive metals [M^{II}TPyzPzPr$_8$(4–)]$^{2-}$ (M = Ni, Pd, Pt, –0.91 - –0.93 V [1]). The formation of dianionic forms of metal phthalocyanines is observed at more negative potentials by 0.2-0.3 V [4].

References

[1] K. Takahashi, Y. Aoki, T. Sugitani, F. Moriyama, Y. Tomita, M. Handa, K. Kasuga, K. Sogabe, *Inorg. Chim. Acta* **1992**, *201*, 247-249.

[2] K. Ohta, T. Watanabe, T. Fujimoto, I. Yamamoto, *J. Chem. Soc., Chem. Commun.* **1989**, 1611-1613.

[3] S. Dong, B. Liu, J. Liu, N. Kobayashi, *J. Porphyrins Phthalocyanines* **1997**, *1*, 333-340.

[4] A. B. P. Lever, E. R. Milaeva, G. Speier The redox chemistry of metallophthalocyanines. In Phthalocyanines: Properties and Applications. Vol. 3, VCH Publishing, Weinheim. Pages 1- 70.

	Cryptand [2,2,2]	{cryptand[2,2,2](Na^+)} $(C_{60})_3^-$ ·$2C_6H_4Cl_2$ (**1**)	{cryptand[2,2,2](Na^+)} $(C_{60})_2^-$ (**2**)	{cryptand[2,2,2](Na^+)}$_8$ $(C_{60})_6^{8-}$ (**3**)	{cryptand[2,2,2](Na^+)}$_2$ $(C_{60}^-)_2$ ·$C_6H_4Cl_2$·C_6H_{14} (**4**)
Cryptand	423w	423w	-	423w	422w
	476w	482w	-	476w	466w
	528w	525s*	526s*	527w*	525w*
	581w	575m*	576s*	574s*	575s*
	735m	-	738w	-	-
	-	746m*	747w	748w	751m*
	922m	924m	932w	933m	932m
	948w	946m	939w	940m	943m
	982m	-	-	-	-
	1038w	1034w*	1032w	1030w	1033w*
	1071m	1077m	-	1080m	-
	1100s	1103s	1103s	1102s	1103s
	1127s	1129m	1134m	1135m	1135m
	1213w	1236w	1242w	1239w	1239w
	1295m	1296m	1298m	1299m	1297m
	1329m	-	-	-	-
	1360s	1355m	1355s	1355s	1353s
	1446m	-	1440w	1440m	-
	1462m	1454m*	1454m	1454m	1455m*
	1490w	1475m	1481w	1480m	1478w
	2790w	2812w	2813w	2794w	2813w

IR- spectra

	2877w	2877w	2875w	2868w	2881w
	-	2914w	-	2919w	2918w
	2943w	2950w	2958w	2958w	2957w
Fullerene		525s*	526s*	527w*	514w
		575m*	576s*	574s*	525w*
		1181w	1182m	1180w	575s*
		1404w	1390s ($C_{60}^{\bullet-}$)	1377m (C_{60}^{2-})	1183w
			1429m(C_{60}^{0})	1386 s ($C_{60}^{\bullet-}$)	1393s ($C_{60}^{\bullet-}$)
Solvent		658w			658w
		746m*			751m*
		1034w*			1033w*
		1454m*			1455m*

Table S1 IR-spectra (cm^{-1} in KBr) of starting compounds and complexes **1-4**.
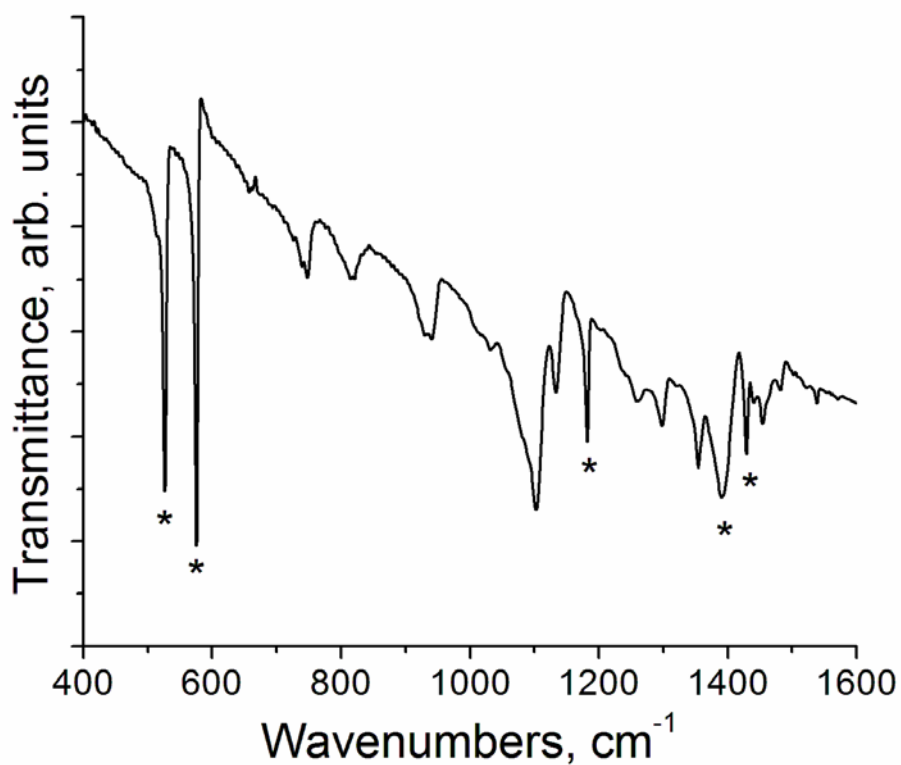
Figure S2. IR-spectrum of {cryptand[2,2,2](Na^{+})}(C$_{60}$)$_{2}^{-}$ (**2**) in KBr pellet prepared in anaerobic conditions. Absorption bands of C$_{60}$ are marked by asterisks.
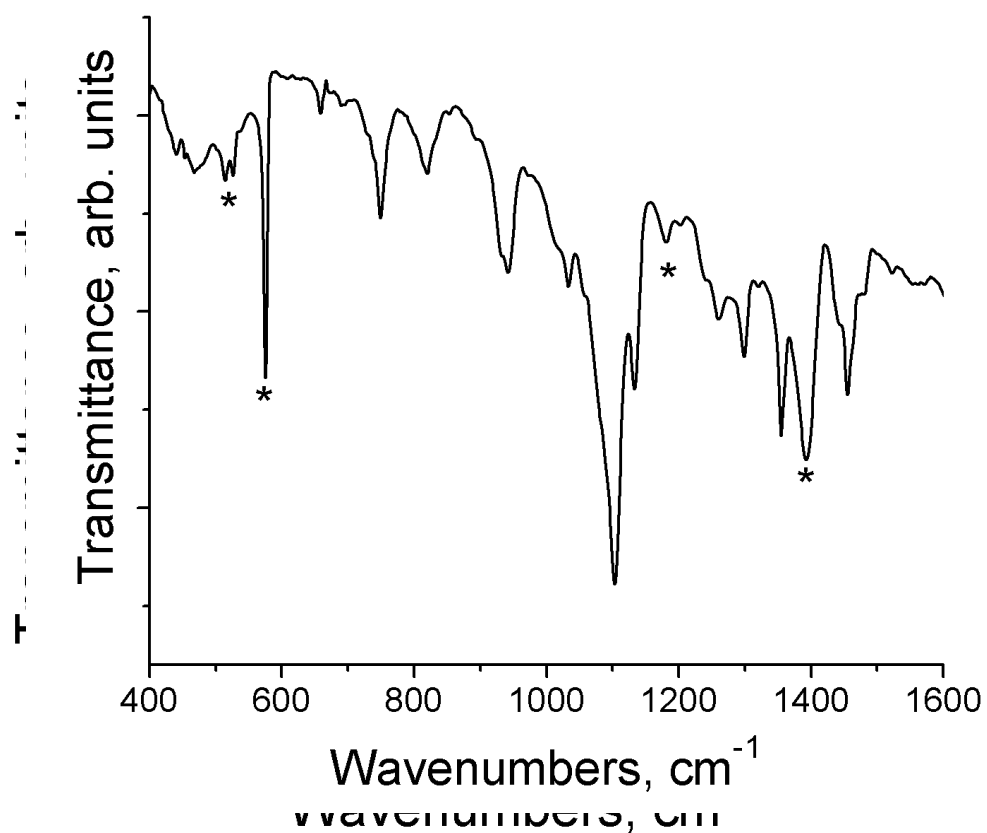
Figure S4. IR-spectrum of {cryptand[2,2,2](Na^+)}$_2$(C_{60}^-)$_2$·$C_6H_4Cl_2$·C_6H_{14} (**4**) in KBr pellet prepared in anaerobic conditions. Absorption bands of C_{60} are marked by asterisks.

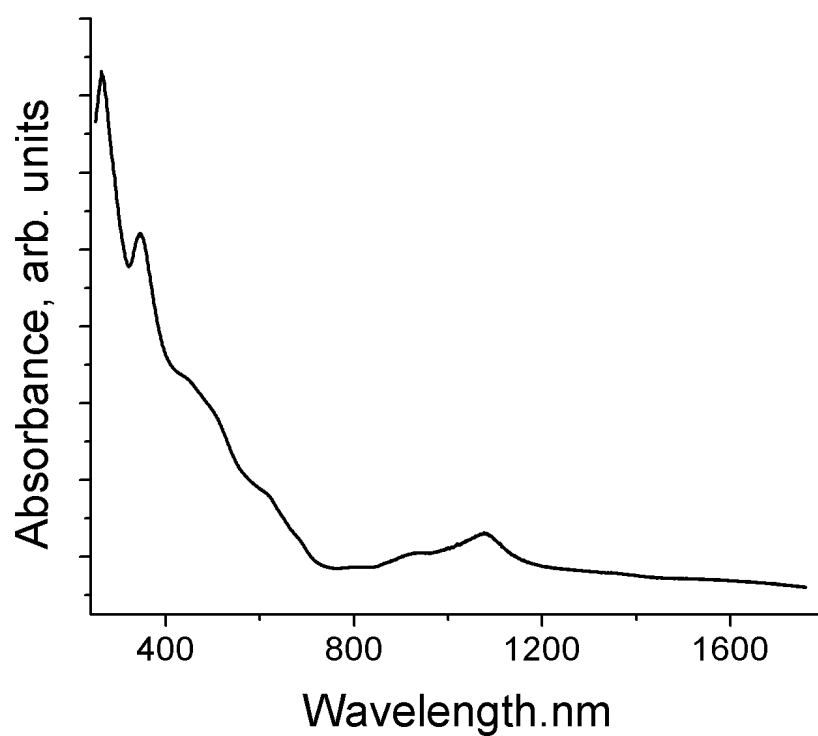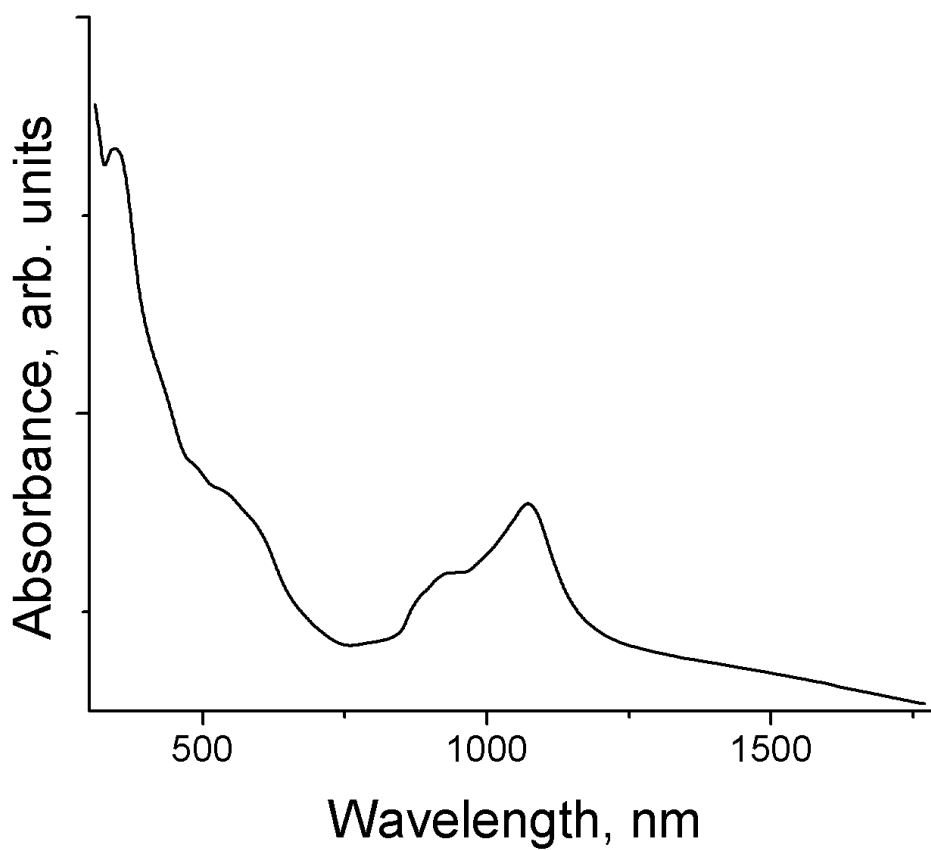**Figure**   · pellet

prepared

Figure S6. UV-visible-NIR spectrum of {cryptand[2,2,2](Na^+)}$_2$$(C_{60}^-)_2$·$C_6H_4Cl_2$·$C_6H_{14}$ (**4**) in